

## A preliminary report of the Yangbi, Yunnan, $M_S$ 6.4 earthquake of May 21, 2021

ZhiGao Yang , Jie Liu , Xue-Mei Zhang , WenZe Deng , GuangBao Du , and XiYan Wu

**Citation:** (2021). A preliminary report of the Yangbi, Yunnan,  $M_S$  6.4 earthquake of May 21, 2021. *Earth Planet. Phys.*, 5(4), 1–3.  
<https://doi.org/10.26464/epp2021036>

---

## Articles you may be interested in

**Geometry and tectonic deformation of the seismogenic structure for the 8 August 2017  $M_S$  7.0 Jiuzhaigou earthquake sequence, northern Sichuan, China**

Earth and Planetary Physics. 2019, 3(3), 253 <https://doi.org/10.26464/epp2019027>

**Anomalous phenomena in DC–ULF geomagnetic daily variation registered three days before the 12 May 2008 Wenchuan  $M_S$  8.0 earthquake**

Earth and Planetary Physics. 2019, 3(4), 330 <https://doi.org/10.26464/epp2019034>

**The 2018  $M_S$  5.9 Mojiang Earthquake: Source model and intensity based on near-field seismic recordings**

Earth and Planetary Physics. 2019, 3(3), 268 <https://doi.org/10.26464/epp2019028>

**Which velocity model is more suitable for the 2017  $M_S$  7.0 Jiuzhaigou earthquake?**

Earth and Planetary Physics. 2018, 2(2), 163 <https://doi.org/10.26464/epp2018016>

**Regional stress field in Yunnan revealed by the focal mechanisms of moderate and small earthquakes**

Earth and Planetary Physics. 2019, 3(3), 243 <https://doi.org/10.26464/epp2019024>

**A test on methods for  $M_C$  estimation based on earthquake catalog**

Earth and Planetary Physics. 2018, 2(2), 150 <https://doi.org/10.26464/epp2018015>



Follow EPP WeChat public account for more information

# A preliminary report of the Yangbi, Yunnan, $M_s6.4$ earthquake of May 21, 2021

ZhiGao Yang<sup>1</sup>, Jie Liu<sup>1\*</sup>, Xue-Mei Zhang<sup>1</sup>, WenZe Deng<sup>1</sup>, GuangBao Du<sup>1</sup>, and XiYan Wu<sup>2</sup>

<sup>1</sup>China Earthquake Networks Center, Beijing 100045, China;

<sup>2</sup>Institute of Geology, Chinese Earthquake Administration, Beijing 100029, China

**Keywords:** Yangbi  $M_s6.4$  earthquake; focal mechanism; earthquake sequence

**Citation:** Yang, Z. G., Liu, J., Zhang, X.-M., Deng, W. Z., Du, G. B. and Wu, X. Y. (2021). A preliminary report of the Yangbi, Yunnan,  $M_s6.4$  earthquake of May 21, 2021. *Earth Planet. Phys.*, 5(4), 362–364. <http://doi.org/10.26464/epp2021036>

According to the reports of China Earthquake Networks Center, an  $M_s6.4$  earthquake occurred in Yangbi City, Dali Prefecture, Yunnan Province, on May 21, 2021; the epicenter was located at 25.67°N and 99.87°E with a focal depth of 8 km. Within 5 km from the epicenter the average elevation is 2268 m.

Seismicity in the Yangbi area is relatively active (Figure 1). Since 1970, 145 earthquakes of magnitude greater than 3.0 have occurred within 50 km, including 108  $M_s3.0$ –3.9 events, 27  $M_s4.0$ –4.9 events, 9  $M_s5.0$ –5.9 events, and the latest one reported here, which, at  $M_s6.0$ –6.9, is the strongest in this 51-year record. In the area within 100 km of Yangbi, 312 earthquakes above magnitude 3 have been recorded since 1970, including 249  $M_s3.0$ –3.9 events, 45  $M_s4.0$ –4.9 events, 16  $M_s5.0$ –5.9 events, and two  $M_s6.0$ –6.9 events; the other  $M_s6.0$  earthquake occurred in Yongsheng, Yunnan, on October 27, 2001.

Between 18h of May 18 and 08h00m of May 26, 2021, 43 earthquakes above  $M_s3.0$  were recorded (Table 1), including the main event of  $M_s6.0$ –6.9, three of  $M_s5.0$ –5.9, 12 of  $M_s4.0$ –4.9, and 27 of  $M_s3.0$ –3.9. The aftershock sequence was distributed in a NW-SE trending belt about 16 km long (Figure 2); the mainshock was at the northwest end of the aftershock zone. The earthquake sequence took place near the south section of the Weixi–Qiaohou Fault, which is an active Holocene fault.

Utilizing the continuous waveform data of the earthquake sequence recorded by 15 nearby broadband seismic stations, and adopting the regional earthquake full waveform fitting method (Herrmann et al., 2011; Herrmann, 2013), we calculated the focal mechanism solutions of the fore-, main-, and after-shocks of magnitude greater than  $M_s4.0$  (Table 2 and Figure 2). Because of the interference of the mainshock coda, waveforms following in at least the first half hour were disturbed; stable focal mechanism solutions could thus not be obtained for them by the waveform fitting method.

Correspondence to: J. Liu, liujie@seis.ac.cn

Received 26 MAY 2021; Accepted 02 JUN 2021.

Accepted article online 04 JUN 2021.

©2021 by Earth and Planetary Physics.

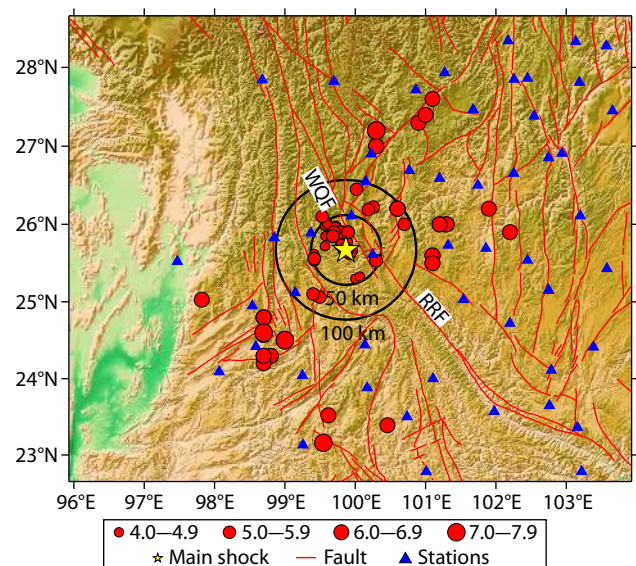


**Figure 1.** Mainshock location and distribution of historical earthquakes since 1970. Only the relatively large events are shown:  $M_s \geq 4.0$  within 50 km from the mainshock,  $M_s \geq 5.0$  within 100 km, and  $M_s \geq 6.0$  within 300 km. RRF: Red River fault; WQF: Weixi–Qiaohou fault.

Based on the observed aftershock activity characteristics and the focal mechanism solutions, we report the following description of this sequence:

(1) According to the  $M$ - $t$  plot of the earthquake sequence (Figure 3) and the epicenter migration  $D$ - $t$  plot (Figure 4) a number of foreshocks occurred in the 4 days before the mainshock, including 4  $M_s4.0$ –4.9 events and one  $M_s5.0$ –5.9 event; the largest foreshock — the  $M_s5.6$  event — occurred 27 minutes before the mainshock. The foreshocks took place mainly to the southeast of, and 5–10 km apart from, the mainshock (Figure 4). Aftershocks were active in the first day after the mainshock, but in the following several days only sporadic  $M_s \geq 3.0$  events took place. The mainshock, a unilateral fracture, was at the northwest end of the aftershock zone. From 8 o'clock, May 22 to 6 o'clock, May 26 the aftershocks migrated from northwest to southeast until an  $M_s3.0$

**Table 1.** Catalog of fore-, main-, and aftershocks.

No.	Time (CST)	Lat. (°N)	Lon. (°E)	Depth (km)	Mag.	Location
1	2021-05-18 18:49:30	25.65	99.93	8	3.2	Yangbi
2	2021-05-18 20:56:46	25.65	99.93	8	3.0	Yangbi
3	2021-05-18 21:39:35	25.65	99.93	8	4.2	Yangbi
4	2021-05-19 03:27:56	25.65	99.92	8	3.1	Yangbi
5	2021-05-19 20:05:56	25.66	99.92	8	4.4	Yangbi
6	2021-05-19 21:13:07	25.68	99.89	8	3.2	Yangbi
7	2021-05-20 01:58:59	25.67	99.90	11	3.2	Yangbi
8	2021-05-21 20:56:02	25.63	99.93	8	4.2	Yangbi
9	2021-05-21 21:21:25	25.63	99.92	10	5.6	Yangbi
10	2021-05-21 21:23:44	25.66	99.97	8	4.5	Yangbi
11	2021-05-21 21:48:35	25.67	99.87	8	6.4	Yangbi
12	2021-05-21 21:53:48	25.62	99.98	9	4.1	Yangbi
13	2021-05-21 21:55:29	25.67	99.89	8	5.0	Yangbi
14	2021-05-21 21:56:38	25.64	99.95	8	4.9	Yangbi
15	2021-05-21 22:02:01	25.66	99.89	8	4.1	Yangbi
16	2021-05-21 22:03:36	25.57	99.93	8	3.9	Yangbi
17	2021-05-21 22:15:16	25.59	99.96	8	4.0	Yangbi
18	2021-05-21 22:19:48	25.60	99.95	8	3.0	Yangbi
19	2021-05-21 22:30:27	25.65	99.90	8	3.1	Yangbi
20	2021-05-21 22:31:11	25.59	99.97	8	5.2	Yangbi
21	2021-05-21 22:59:37	25.63	99.94	8	3.5	Yangbi
22	2021-05-21 23:08:58	25.61	99.98	8	3.0	Yangbi
23	2021-05-21 23:13:54	25.64	99.94	8	3.8	Yangbi
24	2021-05-21 23:18:10	25.62	99.98	8	3.0	Yangbi
25	2021-05-21 23:22:49	25.66	99.88	8	3.5	Yangbi
26	2021-05-21 23:23:35	25.60	99.98	8	4.5	Yangbi
27	2021-05-22 00:24:06	25.69	99.87	8	3.0	Yangbi
28	2021-05-22 00:51:41	25.70	99.87	8	4.0	Yangbi
29	2021-05-22 00:53:31	25.65	99.91	8	3.2	Yangbi
30	2021-05-22 00:56:08	25.63	99.91	9	3.2	Yangbi
31	2021-05-22 01:36:06	25.62	99.94	9	3.5	Yangbi
32	2021-05-22 01:50:18	25.61	100.00	14	3.3	Yangbi
33	2021-05-22 02:24:27	25.66	99.88	10	3.0	Yangbi
34	2021-05-22 02:28:44	25.62	99.91	10	3.9	Yangbi
35	2021-05-22 04:10:57	25.62	99.95	12	3.4	Yangbi
36	2021-05-22 08:36:47	25.68	99.90	12	3.4	Yangbi
37	2021-05-22 09:48:01	25.67	99.90	12	4.0	Yangbi
38	2021-05-22 17:24:16	25.66	99.90	10	3.3	Yangbi
39	2021-05-22 20:14:36	25.61	99.93	10	4.4	Yangbi
40	2021-05-22 22:30:05	25.60	99.93	11	3.2	Yangbi
41	2021-05-24 08:10:58	25.59	100.00	8	3.0	Yangbi
42	2021-05-24 08:43:10	25.59	100.01	8	3.1	Yangbi
43	2021-05-26 06:37:24	25.65	99.89	10	3.0	Yangbi

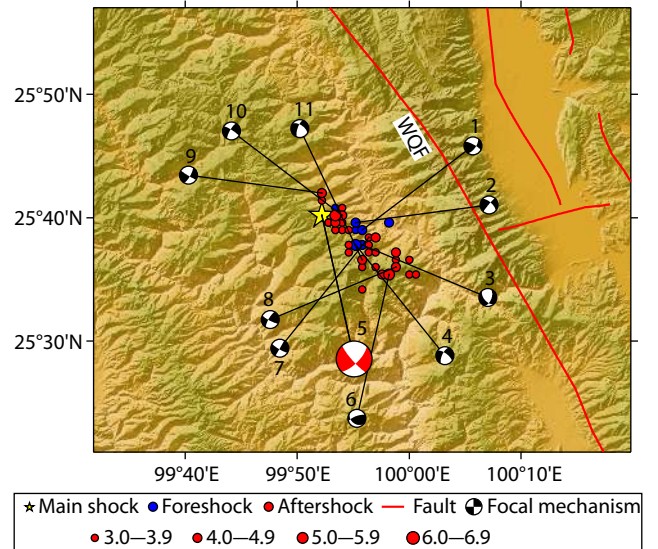


**Figure 2.** The location of the foreshocks (blue), the mainshock (yellow), aftershocks (red) recorded between May 18 and 8h on the 26th, and the focal mechanism solutions of some large events.

**Table 2.** Focal mechanism solutions of fore-, main-, and aftershocks.

No.	Time (CST)	Latitude (°N)	Longitude (°E)	Centroid depth (km)	$M_w$	Focal mechanism planes I and II (strike/dip/rake)(°)
1	2021-5-18 21:39:35	25.65	99.93	8	4.3	35/65/15 299/76/154
2	2021-5-19 20:05:56	25.66	99.92	7	4.6	220/85/-25 312/65/-174
3	2021-5-21 20:56:02	25.63	99.93	6	4.2	20/55/-45 140/55/-135
4	2021-5-21 21:21:25	25.63	99.92	8	5.2	205/65/-25 306/67/-153
5	2021-5-21 21:48:34	25.67	99.87	11	6.0	45/70/-10 138/81/-160
6	2021-5-21 22:31:10	25.59	99.97	11	5.1	250/70/60 129/36/144
7	2021-5-21 23:13:53	25.64	99.94	7	3.9	30/90/-10 120/80/-180
8	2021-5-21 23:23:34	25.60	99.98	6	4.4	210/75/10 117/80/165
9	2021-5-22 00:51:41	25.70	99.87	6	4.2	30/75/-5 121/85/-165
10	2021-5-22 09:48:00	25.67	99.9	6	4.1	210/75/-10 303/80/-165
11	2021-5-22 20:14:36	25.61	99.93	8	4.6	200/70/-35 303/57/-156

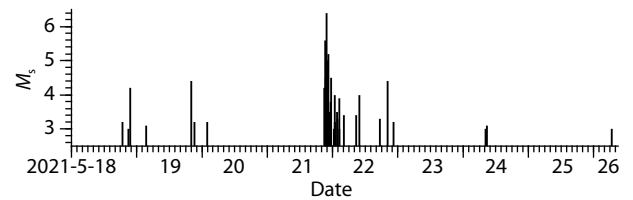


**Figure 3.**  $M-t$  plot of the earthquake sequence (May 18 to 26, 8 o'clock).

earthquake occurred near the mainshock on May 26 (Figure 4).

(2) The moment magnitude of the mainshock is  $M_W 6.0$ ; the strike/dip/rake of the two nodal planes of the optimum double couple model are  $45^\circ/70^\circ/-10^\circ$  and  $138^\circ/81^\circ/-160^\circ$ , respectively, and the latter coincides with the spatial trend of the aftershock distribution and the surface trend of the nearby Weixi–Qiaohou Fault; assuming this fault to be the actual fracture plane, the mainshock therefore took place on a near-vertical strike-slip fault with a small amount of normal faulting.

(3) By waveform fitting, the best centroid depth of the mainshock is 11 km, which is slightly deeper than the initial rupture. Figure 5 shows the centroid depth variation with time for this earthquake sequence. It can be seen that, except for the mainshock, the centroid depths of the foreshocks and aftershocks are mainly between 6 and 8 km; on the whole, the centroid depths are rather shallow and within a narrow range.

(4) Most focal mechanism solutions of this earthquake sequence are generally similar to each other, being mainly of the strike-slip type, similar to that of the mainshock (Table 2). But the focal mechanisms of Event 3 (a foreshock) and Event 6 (the first aftershock) (Table 2) are, respectively, of normal and reverse fault type, which are significantly different from the focal mechanism of the mainshock. In order to verify the reliability of the data, we adopted the jackknife method (Efron and Stein, 1981) and carried out 1000 inversions by random station selection. The result verified the stability of these two focal mechanism solutions. Most earthquakes in Table 2 have a small component of normal faulting (negative rake), indicating that the fault contains a certain portion of normal faulting component. Event 3 is at the southeast end of the foreshock sequence, corresponding to a near NS-trending normal fault. Event 6 is an  $M_s 5.2$  aftershock ( $M_W 5.1$ ), located at the southeast end of the aftershock zone; we conjecture that Event 6 occurred on a near EW-trending secondary reverse fault, which could explain the termination of the aftershock distribution in the southeast direction.

(5) The focal mechanisms of the earthquake sequence (except for Event 3 in Table 2) indicate that the maximum principal stress axis is nearly in the NS direction, slightly biased towards the west, which agrees with the regional stress field and ground surface deformation observations (Zheng G et al., 2017; Xu Y et al., 2020). These findings indicate that the seismogenic fault is controlled by the regional stress field.

In summary, this earthquake sequence is of the fore-main-aftershock type. Aftershock activities were rather strong, but occurred mainly within one day of the mainshock, after which occurred only sporadic  $M_s \geq 3.0$  earthquakes. Beginning at 8 o'clock, May 22, the earthquakes migrated towards the southeast, then returned to the vicinity of the May 21 mainshock. The mainshock occurred on a steep strike-slip fault, which contains a small normal fault component; the Weixi–Qiaohou Fault near the earthquake sequence is probably the seismogenic fault. Most focal mechanism solutions of the sequence are consistent with that of the mainshock. The exception is an aftershock in the southeast section, which is of the reverse type; it occurred on a fault that may terminate the aftershocks in the SE direction. The  $P$  axes of most focal mechanism solutions of the sequence are approximately in

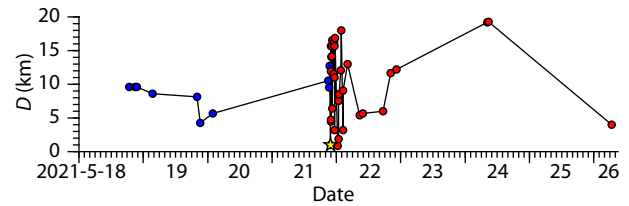


**Figure 4.**  $D$ - $t$  plot of earthquake migration (May 18 to 26, 8 o'clock). The ordinate  $D$  represents the distance of earthquake projection onto the trend line, which is calculated as follows. First find a trend line crossing the earthquake sequence distribution, which is generally the major axis (N138E) of the aftershock zone, so the distance sum of all events to this line is the minimum. Draw perpendicular lines from the earthquakes to the trend line,  $D$  is the distance between the foot of an event and the foot of the mainshock; set the  $D$  of the mainshock as 0. In the plot, 1 km is added to all  $D$ s of the sequence so the mainshock symbol is not cut by the abscissa.

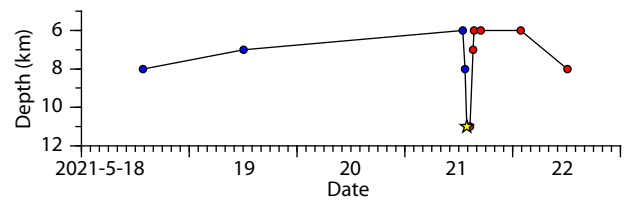


**Figure 5.** Earthquake centroid depth (Table 2) variation with time.

the NS direction, which tallies with the regional stress field and ground deformation observations, indicating that the seismogenic fault is under the control of the regional stress field. The centroid depths from the mechanism solutions are distributed in a narrow range (6–11 km), indicating that the aftershocks took place mainly in a rather shallow part of the fault.

## Acknowledgments

The seismic data were provided by China Earthquake Networks Center. We are grateful for products and services provided by the workgroup on earthquake emergency data products and services. This work was sponsored by the National Key R&D Program on Monitoring, Early Warning and Prevention of Major Natural Disaster (2017YFC1500304).

## References

- Efron, B. and Stein, C. (1981). The jackknife estimate of variance. *Ann. Stat.*, 9(3), 586–596.
- Herrmann, R. B., Malagnini, L., and Munafò, I. (2011). Regional moment tensors of the 2009 L'aquila earthquake sequence. *Bull. Seismol. Soc. Am.*, 101(3), 975–993. <https://doi.org/10.1785/0120100184>
- Herrmann, R. B. (2013). Computer programs in seismology: an evolving tool for instruction and research. *Seismol. Res. Lett.*, 84(6), 1081–1088. <https://doi.org/10.1785/0220110096>
- Xu, Y., Koper, K. D., Burlacu, R., Herrmann, R. B., and Li, D. N. (2020). A New uniform moment tensor catalog for Yunnan, China, from January 2000 through December 2014. *Seismol. Res. Lett.*, 91(2A), 891–900. <https://doi.org/10.1785/0220190242>
- Zheng, G., Wang, H., Wright, T. J., Lou, Y. D., Zhang, R., Zhang, W. X., Shi, C., Huang, J. F., and Wei, N. (2017). Crustal deformation in the India-Eurasia collision zone from 25 years of GPS measurements. *J. Geophys. Res.: Solid Earth*, 122(11), 9290–9312. <https://doi.org/10.1002/2017JB014465>